

Behavior of PtPb/MgAl₂O₄ catalysts with different Pb contents and trimetallic PtPbIn catalysts in *n*-butane dehydrogenation

Sonia A. Bocanegra*, Osvaldo A. Scelza, Sergio R. de Miguel

Instituto de Investigaciones en Catálisis y Petroquímica (INCAPE), Facultad de Ingeniería Química, Universidad Nacional del Litoral – CONICET, Santiago del Estero 2654, 3000 Santa Fe, Argentina

ARTICLE INFO

Article history:

Received 16 April 2013

Received in revised form 15 July 2013

Accepted 23 July 2013

Available online xxx

Keywords:

Olefins

PtPb catalyst

PtPbIn catalysts

Dehydrogenation

ABSTRACT

The behavior of PtPb/MgAl₂O₄ catalysts in butenes production through the *n*-butane dehydrogenation has shown that at low contents, the Pb acts as promoter, improving the conversion and selectivity, whereas at higher contents it has a poisoning effect on the catalytic activity. The PtPb(0.25 wt%)/MgAl₂O₄ catalyst showed the maximum yield to butenes. The characterization results of PtPb catalysts displayed that at low Pb contents there are both dilution and electronic effects of Pb on the Pt sites. On the other hand, at high Pb contents, there is a strong blocking effect of the Pb on the active sites of Pt. In order to study the effect of the In addition in different sequences to PtPb(0.25 wt%)/MgAl₂O₄ catalyst, two catalysts were prepared: PtPb(0.25 wt%)/In(0.28 wt%)/MgAl₂O₄ and PtIn(0.28 wt%)/Pb(0.25 wt%)/MgAl₂O₄. The first catalyst did not show significant advantages with respect to the catalytic behavior of the PtPb(0.25 wt%)/MgAl₂O₄, but the second trimetallic catalyst displayed an increase of both the conversion and the selectivity. The characterization results indicated similar effects of blocking and dilution of promoters on the active sites of Pt for both trimetallic catalysts, but the best catalyst, PtIn(0.28 wt%)/Pb(0.25 wt%)/MgAl₂O₄, showed the highest percentages of In^δ and Pb^δ, thus indicating stronger interaction between Pt, Pb and In.

© 2013 Elsevier B.V. All rights reserved.

1. Introduction

Catalytic alkanes dehydrogenation for the alkenes production has been in commercial use 80 years ago [1]. Pt-based catalysts are known to be very active for different reactions of interest in petrochemistry and fine chemistry, like hydrogenations, dehydrogenations, naphtha reforming, etc. Materials used as a support of these Pt catalysts influence the catalytic behavior. Since acidic supports like Al₂O₃ (very used in naphtha reforming) [2,3], favor the alkanes cracking (undesirable reaction), other materials like Al₂O₃ doped with alkaline metals [4,5], and magnesium and zinc spinels [6,7] have been developed for alkanes dehydrogenation reaction. MgAl₂O₄ is a material with suitable properties to be used as a support of metallic catalysts, such as a high thermal stability, low acidic character, hydrophobic properties and good interaction with the metallic phase [8,9].

For several decades, the effect of adding metallic promoters to the Pt catalysts has been studied. In general, the addition of metallic promoters to Pt catalysts improves the catalytic properties. Specifically, in the alkanes dehydrogenation, a very endothermic reaction, the function of the metallic promoters added to Pt is to decrease

the activities of undesirable reactions, like hydrogenolysis, cracking and coke formation, and hence to increase the selectivity to alkenes and to reduce the catalyst deactivation. Elements of 13 and 14 groups have been studied as good metallic promoters of Pt, mainly Sn, and also other elements such as Ge, In, and Ga [9–14]. Another metal of 14 Group, Pb, has been less studied as a promoter [15–17]. Although Pb and Sn have very similar properties (electronegativity, electronic configuration, atomic volume, first ionization potential), Pb is known to be a notorious poison for Pt catalyst [17,18]. In spite of this, we decided to study the influence of the addition of increasing amounts of Pb to Pt/MgAl₂O₄ catalyst on the catalytic behavior in the production of butenes from the *n*-butane dehydrogenation. New and interesting catalytic results were found for this bimetallic couple.

This work was completed with the preparation, characterization and evaluation of trimetallic catalysts with Pt, Pb and In. It must be taken into account the originality of the study of these trimetallic catalysts, since no studies were found in the literature.

2. Experimental

MgAl₂O₄ was prepared by a solid phase reaction between MgO (Alfa Aesar, purity 99.99%) and γ-Al₂O₃ (CK 300 from Cyanamid Ketjen, purity 99.9%). The steps involved in the preparation of the support were: (a) an intimate mixture of the reactants in the

* Corresponding author. Tel.: +54 342 4555279; fax: +54 342 4531068.
E-mail address: sbocane@fiq.unl.edu.ar (S.A. Bocanegra).

stoichiometric ratio ($\text{MgO}/\gamma\text{-Al}_2\text{O}_3$ molar ratio = 1), (b) grinding of the mixture to obtain a very fine powder using a mortar (the particle size of the obtained powder was smaller than $105\ \mu\text{m}$), (c) formation of a paste by addition of distilled water to the powder, (d) drying at $100\ ^\circ\text{C}$ for 12 h, (e) calcination in an electric furnace at $900\ ^\circ\text{C}$ for 24 h, (f) grinding of the solid to particle sizes between 177 and $500\ \mu\text{m}$ (35–80 mesh) and, finally, (g) purification with $(\text{NH}_4)_2\text{CO}_3$ 1 M solution in order to eliminate the residual MgO in the synthesized solid [8]. The BET surface area of the MgAl_2O_4 was $30\ \text{m}^2\ \text{g}^{-1}$ [8].

All catalysts were prepared by incipient impregnation of the support with an aqueous solution of the metallic precursors and the impregnating volume/weight of support ratio was $1.4\ \text{mL}\ \text{g}^{-1}$. The Pt (0.3 wt%)/ MgAl_2O_4 catalyst was prepared by impregnation of the MgAl_2O_4 with an aqueous solution of H_2PtCl_6 at room temperature for 6 h. The Pt concentration in the solution was $2.14\ \text{g}\ \text{L}^{-1}$. Then the sample was dried at $100\ ^\circ\text{C}$ for 12 h.

PtPb bimetallic catalysts were obtained by impregnation of the corresponding monometallic one with an aqueous solution of $\text{Pb}(\text{NO}_3)_2$ at room temperature for 6 h. The Pb contents were 0.1, 0.25, 0.52 and 0.87 wt%. The concentrations of $\text{Pb}(\text{NO}_3)_2$ were $0.7\ \text{g}\ \text{L}^{-1}$ (0.1 wt%), $1.8\ \text{g}\ \text{L}^{-1}$ (0.25 wt%), $3.8\ \text{g}\ \text{L}^{-1}$ (0.52 wt% Pb) and $6.2\ \text{g}\ \text{L}^{-1}$ (0.87 wt% Pb). After impregnation, the catalysts were dried at $100\ ^\circ\text{C}$ for 12 h, and then calcined under flowing air at $500\ ^\circ\text{C}$ for 3 h.

Trimetallic Pt(0.3 wt%)Pb(0.25 wt%)In(0.28 wt%)/ MgAl_2O_4 catalyst was obtained by impregnation of the bimetallic Pt(0.3 wt%)Pb(0.25 wt%)/ MgAl_2O_4 catalyst (without calcination stage) with an aqueous solution of $\text{In}(\text{NO}_3)_3$ at $25\ ^\circ\text{C}$ for 6 h. Besides trimetallic Pt(0.3 wt%)In(0.28 wt%)Pb(0.25 wt%)/ MgAl_2O_4 catalyst was prepared by impregnation of the Pt(0.3 wt%)/ MgAl_2O_4 catalyst with an aqueous solution of $\text{In}(\text{NO}_3)_3$ at $25\ ^\circ\text{C}$ for 6 h. After impregnation, the catalyst was dried at $100\ ^\circ\text{C}$ for 12 h, and, then, the Pt(0.3 wt%)In(0.28 wt%)/ MgAl_2O_4 catalyst obtained was impregnated with aqueous solution of $\text{Pb}(\text{NO}_3)_2$ (concentration = $1.8\ \text{g}\ \text{L}^{-1}$). For both trimetallic catalysts, the In concentration in the impregnating solution was $2\ \text{g}\ \text{L}^{-1}$. Finally, after impregnation, both catalysts were dried at $100\ ^\circ\text{C}$ overnight and calcined in air at $500\ ^\circ\text{C}$ for 3 h.

n-Butane dehydrogenation reaction was carried out in a quartz continuous flow reactor heated by an electric furnace at $530\ ^\circ\text{C}$ for 2 h. In this case, the reactor (with a catalyst weight of $0.200\ \text{g}$) was fed with $18\ \text{mL}\ \text{min}^{-1}$ of the reactive mixture (*n*-butane and hydrogen, $\text{H}_2/n\text{-C}_4\text{H}_{10}$ molar ratio = 1.25). The reactive mixture was prepared “in situ” by using mass flow controllers. *n*-butane and H_2 (used for the previous reduction of catalysts and for the reaction) were high purity ones (>99.99%). Prior to the reaction, catalysts were reduced “in situ” at $530\ ^\circ\text{C}$ under flowing H_2 for 3 h. The reactor effluent was analyzed in a GC-FID equipment with a packed column ($0.00318\ \text{m} \times 6\ \text{m}$, 20 wt% BMEA on Chromosorb P-AW 60/80), which was kept at $50\ ^\circ\text{C}$ during the analysis. With this analytical device, the amounts of methane, ethane, ethylene, propane, propylene, *n*-butane, 1-butene, *cis*-2-butene, *trans*-2-butene and 1,3-butadiene were measured. The *n*-butane conversion was calculated as the sum of the percentages of the chromatographic areas of all the reaction products (except H_2) corrected by the corresponding response factor. The selectivity to the different reaction products (*i*) was defined as the ratio: mol of product *i*/ \sum mol of all products (except H_2). Taking into account the high temperatures used for the reaction (for thermodynamic reasons), it was necessary to determine the contribution of the homogeneous reaction. For this purpose, a blank experiment was performed by using a quartz bed and the results showed a negligible *n*-butane conversion (<<1%).

Test reaction of the metallic phase, cyclohexane dehydrogenation (CHD), was carried out in a differential flow reactor with

volumetric flow of $6\ \text{mL}\ \text{h}^{-1}$. Prior to this reaction, samples were reduced “in situ” with H_2 at $500\ ^\circ\text{C}$ for 3 h. In this reaction the H_2 /hydrocarbon molar ratio was 26 and the reaction temperature was $300\ ^\circ\text{C}$. The activation energy in CHD for different catalysts was obtained by measuring the initial reaction rate at 270, 285 and $300\ ^\circ\text{C}$. The sample weight was chosen so that the conversion ranged between 1 and 7%. Deactivation of the samples was not observed during the experiments.

Another test reaction of the metallic phase, cyclopentane hydrogenolysis (CPH), was carried out in a differential flow reactor with volumetric flow of $6\ \text{mL}\ \text{h}^{-1}$. Prior to this reaction, samples were reduced “in situ” with H_2 at $500\ ^\circ\text{C}$ for 3 h. In this reaction the H_2 /hydrocarbon molar ratio was 26 and the reaction temperature was $500\ ^\circ\text{C}$. The sample weight was chosen so that the conversion was lower than 7%.

TPR experiments were performed in a quartz flow reactor. The samples were heated at $6\ ^\circ\text{C}\ \text{min}^{-1}$ from room temperature up to about $600\ ^\circ\text{C}$. The reductive mixture (5% v/v $\text{H}_2\text{-N}_2$) was fed to the reactor with a flow rate of $10\ \text{mL}\ \text{min}^{-1}$. Catalysts were previously calcined “in situ” in air at $500\ ^\circ\text{C}$ for 3 h.

XPS measurements were carried out in a VG-Microtech Multilab spectrometer, which operates with an energy power of 50 eV (radiation $\text{MgK}\alpha$, $h\nu = 1253.6\ \text{eV}$). The pressure of the analysis chamber was kept at 4.10×10^{-10} torr. Samples were previously reduced “in situ” at $500\ ^\circ\text{C}$ with H_2 for 2 h. Binding energies (BE) were referred to the C1s peak at 284.9 eV. The peak areas were estimated by fitting the experimental results with Lorentzian–Gaussian curves.

H_2 chemisorption measurements were made in volumetric equipment. The sample was heated under flowing H_2 ($60\ \text{mL}\ \text{min}^{-1}$) from room temperature up to $500\ ^\circ\text{C}$, and then kept at this temperature for 4 h. Then, the sample was outgassed under vacuum (10^{-4} torr) for 1 h. After the sample was cooled down to room temperature ($25\ ^\circ\text{C}$), the hydrogen dosage was performed in the range of 50–250 torr. The chemisorbed hydrogen was calculated by extrapolation of the isotherms to pressure zero.

TEM measurements were carried out on a JEOL 100CX microscope with a nominal resolution of 0.6 nm, operated with an acceleration voltage of 100 kV, and magnification ranges of $80,000\times$ and $100,000\times$. The samples were prepared by grinding, suspending and sonicating them in ethanol, and putting a drop of the suspension on a carbon copper grid. After evaporation of the solvent, the specimens were introduced into the microscope column. For each catalyst, a very important number of Pt particles were observed and the distribution curves of particle sizes were done. The mean metallic particle diameter (*D*) was calculated as: $D = (\sum n_i \cdot d_i) / (\sum n_i)$, where n_i is the number of particles of diameter d_i .

3. Results and discussion

3.1. Evaluation of PtPb catalysts in *n*-butane dehydrogenation reaction

Figs. 1 and 2 show the *n*-butane conversion and the selectivity to all butenes (1-butene, 2-*cis*-butene, 2-*trans*-butene and 1,3-butadiene), respectively, for Pt and PtPb catalysts. The *n*-butane conversion (Fig. 1) shows clearly that the addition of 0.1 wt% and 0.25 wt% of Pb to the Pt catalyst strongly increases the initial conversion with respect to the monometallic one. However, the catalysts with higher Pb contents (0.52 and 0.87 wt%) display lower initial activities than the Pt catalyst. This decrease of the initial activity is very marked for the PtPb(0.87 wt%)/ MgAl_2O_4 catalyst.

The values corresponding to the deactivation parameter (ΔX) along the reaction time (defined as: $\Delta X = [(X_0 - X_f) \times 100 / X_0]$, where X_0 , at 10 min, and X_f , at 120 min, are the initial and the final

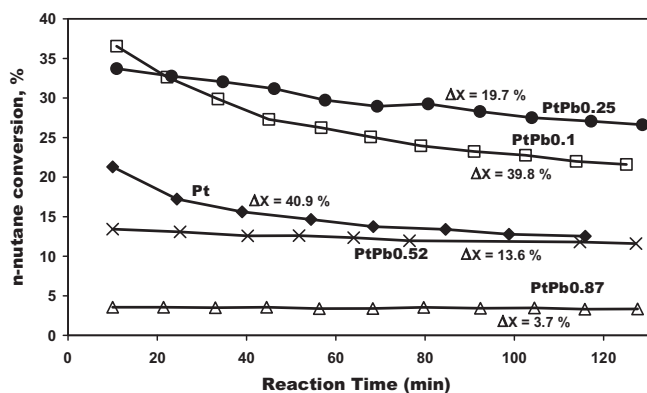


Fig. 1. Values of *n*-butane conversion (*X*) vs. reaction time and deactivation parameter (ΔX), obtained from flow experiments for Pt and PtPb catalysts supported on MgAl_2O_4 .

conversions respectively) are also included in Fig. 1. This deactivation along the reaction time is caused by the carbon formation in the different catalysts. It can be observed similar ΔX values for Pt/ MgAl_2O_4 and PtPb(0.1 wt%)/ MgAl_2O_4 catalysts, whereas for PtPb(0.25 wt%)/ MgAl_2O_4 the deactivation parameter is the half of that of the Pt catalyst. This means that Pb addition to Pt produces a pronounced decrease of the deactivation parameter and hence a lower carbon formation along the reaction time. The catalysts with higher Pb contents (0.52 and 0.87 wt%) show the lowest values of ΔX , though this fact can be also due to the low initial activity of these catalysts.

The selectivity to butenes shows similar values between 92 and 97%, for PtPb(0.25 wt%)/ MgAl_2O_4 and PtPb(0.52 wt%)/ MgAl_2O_4 catalysts, while PtPb(0.1 wt%)/ MgAl_2O_4 displays an initial selectivity of 88% and a final selectivity of 94% (Fig. 2). These values are higher than that for the Pt/ MgAl_2O_4 catalyst. The PtPb(0.87 wt%)/ MgAl_2O_4 catalyst (with very low activity) displays values of selectivities to butenes similar to those of the monometallic catalyst. Besides, the selectivity to butenes for a determined bimetallic catalyst slightly increases with the reaction time, such as Fig. 2 shows, and it is due to the formation of carbon on the more hydrogenolytic sites, thus producing a decrease in the production of the C_1 – C_3 products and hence an increase of the selectivity to the olefins.

In order to understand the influence of the different Pb contents on the catalytic behavior in the *n*-butane dehydrogenation, graphs of yield to butenes (product of the *n*-butane conversion and the selectivity to butenes) were drawn as a function of the Pb/Pt molar ratio of the bimetallic catalysts, and they are shown in Fig. 3. As it can be observed, the catalysts with Pb contents of 0.1 wt% and

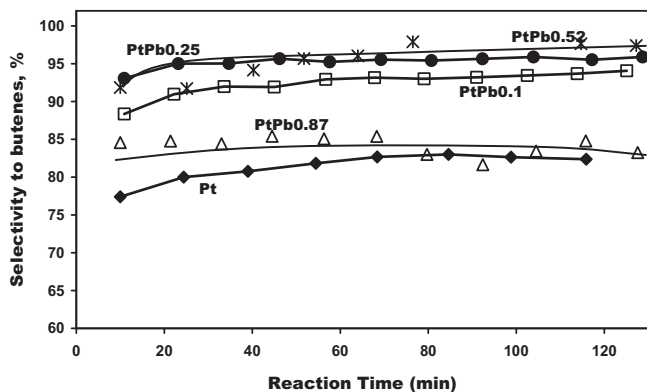


Fig. 2. Selectivity to all butenes (1-butene, cis- and trans-2-butenes, and 1,3-butadiene) vs. reaction time for Pt and PtPb catalysts supported on MgAl_2O_4 .

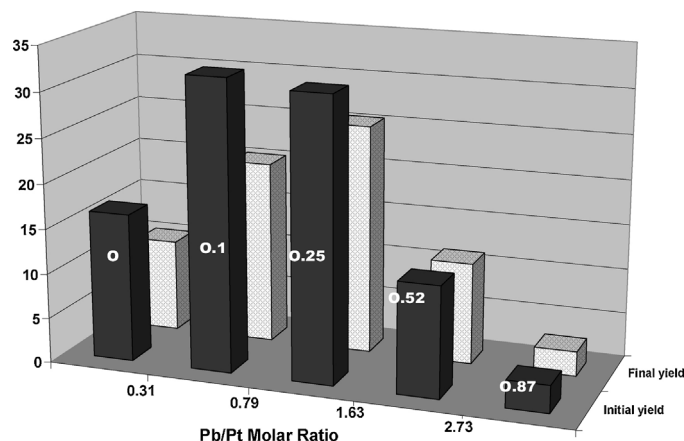


Fig. 3. Initial and final yields to butenes of Pt and PtPb catalysts as a function of the Pb/Pt molar ratio. White numbers on the bars represent the Pb weight percent of catalysts.

0.25 wt% (Pb/Pt molar ratio of 0.31 and 0.79 respectively) have initial and final yields higher to that of the Pt/ MgAl_2O_4 catalyst (initial yield of 16.5% and final yield of 10.3%). On the other hand, catalysts with higher lead contents (0.52 and 0.87 wt%, corresponding to Pb/Pt molar ratios of 1.63 and 2.73, respectively) display initial and final yields similar or lower than that of the monometallic sample. In fact, PtPb(0.1 wt%)/ MgAl_2O_4 catalyst has an initial yield of 32.3% and a final yield of 20.3%, while the catalyst with 0.25 wt% of Pb, has an initial yield of 31.4% and a final one of 25.5%. Hence this last catalyst shows the best catalytic performance since it maintains a high yield along the reaction time. In conclusion there would be an optimum Pb/Pt molar ratio, near 0.79, to achieve the maximum catalytic yield in this reaction.

3.2. Characterization of metallic phase of PtPb catalysts

The measurements of H_2 chemisorption for the different PtPb/ MgAl_2O_4 catalysts are displayed in Table 1. For low Pb contents (0.1 and 0.25 wt%), no significant changes were observed with respect to the Pt catalyst. On the other hand, at high Pb contents (0.52 and 0.87 wt%), a strong fall in the H_2 chemisorption values is displayed. This phenomenon could be attributed to the presence of geometric and/or electronic effects of the Pb atoms on the Pt sites or to an important growth in the size of the metallic particles. In order to analyze the probable modification of the sizes of the particles, Fig. 4 shows the distribution of particles sizes determined by TEM for a mono and bimetallic PtPb catalysts. These TEM results (Fig. 4) indicate that there are no significant changes in the size of

Table 1

Results of H_2 chemisorption, initial rates (R_{CH}^0) and activation energies (E_{CH}) in CHD, and initial rates (R_{CP}^0) in CPH for all catalysts.

Catalysts	H_2 chemisorp. ($\mu\text{mol H}_2 \text{ g cat}^{-1}$)	CHD (300 °C)		CPH (500 °C)
		R_{CH}^0	E_{CH}	R_{CP}^0
Pt/ MgAl_2O_4	3.75	62.7	23.8	5.7
PtPb(0.1)/ MgAl_2O_4	3.97	38.0	27.4	2.2
PtPb(0.25)/ MgAl_2O_4	3.62	22.8	29.0	1.2
PtPb(0.52)/ MgAl_2O_4	0.62	10.9	14.5	1.0
PtPb(0.87)/ MgAl_2O_4	0.28	7.0	11.0	0.8
PtPb(0.25)In(0.28)/ MgAl_2O_4	1.96	4.9	n.d.	0.7
Pt In(0.28)Pb(0.25)/ MgAl_2O_4	1.84	3.6	n.d.	1.1

R_{CH}^0 : mol CH g Pt $^{-1}$ h $^{-1}$.

R_{CP}^0 : mol CP g Pt $^{-1}$ h $^{-1}$.

E_{CH} : Kcal mol CH $^{-1}$.

n.d.: not determined.

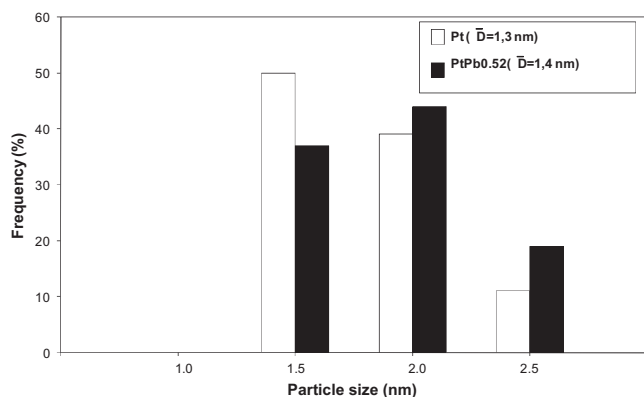


Fig. 4. Distribution of metallic particle sizes by TEM for Pt and PtPb catalysts.

the metallic particles by Pb addition to the Pt catalyst, since the average diameter of metallic particles is 1.3 nm for the Pt/MgAl₂O₄ catalyst and 1.4 nm for the PtPb(0.52 wt%)/MgAl₂O₄ one.

To study the presence of geometric and/or electronic effects, test reactions of the metallic phase were carried out. Results of the test reactions, cyclohexane dehydrogenation (CHD) and cyclopentane hydrogenolysis (CPH), for mono and bimetallic catalysts are presented in Table 1. By comparing CHD results of bimetallic catalysts with that of the monometallic Pt catalyst, it can be observed a moderate decrease of the initial rate (R_{CH}°) for the catalysts with Pb contents of 0.1 and 0.25 wt%. At the same time, in these catalysts it is observed an increase of the activation energy (E_{CH}). In contrast to these results, the catalysts with Pb contents of 0.52 and 0.87 wt% show a strong decrease of R_{CH}° (decrease of 83–89%) respect to the monometallic catalyst. Besides, these catalysts display a decrease of the E_{CH} respect to that of Pt catalyst. Taking into account that the cyclohexane dehydrogenation reaction is a facile or structure-insensitive reaction [19], the important increase of the activation energy in PtPb(0.1 wt%) and PtPb(0.25 wt%) catalysts with respect to the monometallic one indicates that at low Pb contents there are electronic effects of Pb atoms on the Pt sites. On the other hand, at high Pb contents, the decrease of the initial rate and of the activation energy would be due mainly to a blocking effect of Pb on Pt surface atoms, as it was found by Gonzalez-Marcos et al. [20] for PtSn/Al₂O₃ catalysts with very high Sn contents.

Table 1 also shows that the addition of Pb to the Pt catalyst decreases the cyclopentane hydrogenolysis activity, a structure-sensitive reaction carried out on ensembles of active sites [21]. In this sense, a strong decrease (62%) of the initial rate (R_{CP}°) is observed when low amounts of Pb are added to the Pt catalyst. For higher Pb contents, a gradual decrease in R_{CP}° is displayed. At low Pb contents (0.1 and 0.25 wt%), electronic effects of the promoter on Pt sites and a dilution of the active metal by Pb would be the predominating effects. On the other hand, for PtPb(0.52 wt%)/MgAl₂O₄ and PtPb(0.87 wt%)/MgAl₂O₄ catalysts the presence of geometric effects (dilution and blocking) of Pb atoms on Pt sites, would justify the behavior in CPH.

TPR results of PtPb catalysts are shown in Fig. 5. The main reduction peak of Pt in Pt/MgAl₂O₄ sample appears at 230 °C. This peak is shifted to higher temperatures and it becomes broader when increasing Pb amounts are added to the monometallic catalyst, which indicates a Pt–Pb co-reduction and a good interaction of Pt with the second metal. Besides, in both bimetallic catalysts, it can be observed a small reduction zone at high temperatures which can be attributed to the reduction of small quantities of isolated Pb species stabilized on the support.

XPS values were taken as a correct measurement of the final oxidation state of Pb in the catalysts after reduction at high temperature. It must be noted that in all catalysts, only metallic Pt

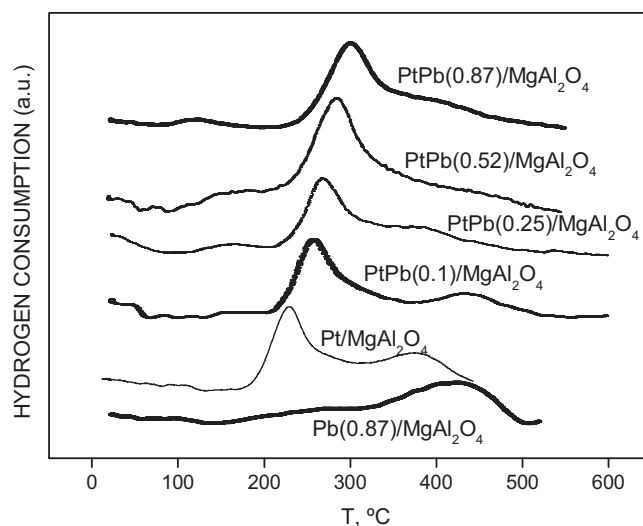


Fig. 5. TPR profiles of calcined Pt, Pb and PtPb catalysts supported on MgAl₂O₄.

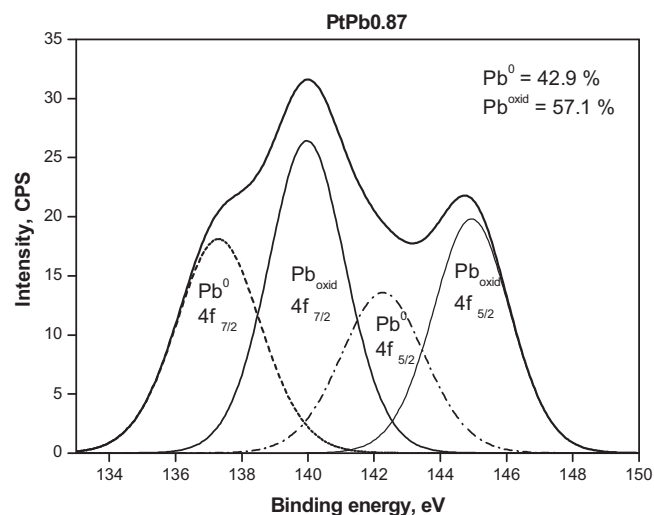


Fig. 6. XPS spectra corresponding to the Pb 4f level for PtPb(0.87 wt%)/MgAl₂O₄ catalyst, previously reduced at 500 °C.

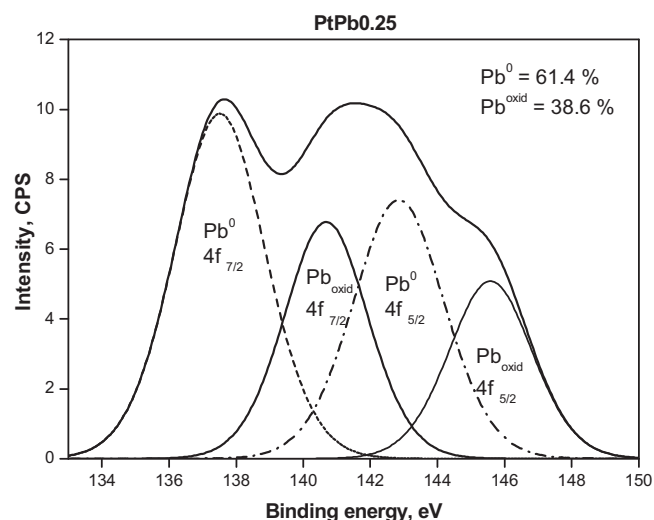


Fig. 7. XPS spectra corresponding to the Pb 4f level for PtPb(0.25 wt%)/MgAl₂O₄ catalyst, previously reduced at 500 °C.

Table 2
Results of XPS for bi and trimetallic catalysts.

Catalysts	Binding energy Pb 4f _{7/2} (eV)	Binding energy In 3d _{5/2} (eV)	Surface molar ratio Pb/Pt	Surface molar ratio In/Pt
PtPb(0.25 wt%)/MgAl ₂ O ₄	137.6(61.4%) 139.3(38.6%)		2.0	
Pt Pb(0.87 wt%)/MgAl ₂ O ₄	137.3(42.9%) 140.0(57.1%)		8.2	
PtPb(0.25 wt%)In(0.28 wt%)/MgAl ₂ O ₄	137.7(53.1%) 140.7(46.9%)	4436 (82.6%) 4452 (17.4%)	1.3	0.9
PtIn(0.28 wt%)Pb(0.25 wt%)/MgAl ₂ O ₄	137.6(65.0%) 139.6(35.0%)	443.1 (100%)	1.9	1.1

Bulk molar ratio Pb/Pt(0.87 wt% of Pb) = 2.7.

Bulk molar ratio Pb/Pt(0.25 wt% of Pb) = 0.8.

Bulk molar ratio In/Pt(0.28 wt% of In) = 1.6.

was found by XPS analysis (Pt 4d signal). The deconvolutions of Pb 4f signal obtained by XPS for PtPb(0.87 wt%)/MgAl₂O₄ and PtPb(0.25 wt%)/MgAl₂O₄ catalysts are displayed in Figs. 6 and 7, respectively. In both graphs four peaks can be observed. The two first ones correspond to the Pb 4f_{7/2} signal, while the two last ones correspond to the Pb 4f_{5/2} signal. For the PtPb(0.87 wt%)/MgAl₂O₄ catalyst, the first peak at a binding energy of 137.3 eV is assigned to the zerovalent Pb, and the second peak at 140 eV corresponds to Pb oxide, according to bibliography [22]. The third (142.3 eV) and fourth (145 eV) peaks correspond to Pb zerovalent and Pb oxide, respectively [21,23]. The PtPb(0.25 wt%)/MgAl₂O₄ catalyst also shows four peaks. The two first ones correspond to Pb zerovalent (137.6 eV) and Pb oxide (139.3 eV), respectively for the Pb 4f_{7/2} signal, and the two last ones (Pb 4f_{5/2}) are assigned to Pb zerovalent (143 eV) and Pb oxide (145.6 eV), respectively. Table 2 summarizes the XPS results for bi and trimetallic catalysts. The bimetallic PtPb catalyst with the highest Pb content (0.87 wt%) presents the higher percentage of Pb oxide (57%), such as it was observed in Table 2. Besides, this catalyst also presents the highest Pb/Pt surface molar ratio (8.2). Even though it was found a surface enrichment in Pb in both PtPb catalysts, such as it was detected by Cheung et al. [18] this phenomenon is more pronounced in PtPb(0.87 wt%)/MgAl₂O₄ catalyst. With respect to the PtPb(0.25 wt%)/MgAl₂O₄ catalyst, it was observed a higher reducibility to metallic Pb (61%), which could be related to higher interaction between both metals, in agreement with other characterization results.

For a detailed analysis of characterization results and catalytic behavior in *n*-butane dehydrogenation of bimetallic catalysts, Fig. 8 shows all the results as a function of the Pb/Pt molar ratio. Geometric effects (dilution and blocking) were studied through the values

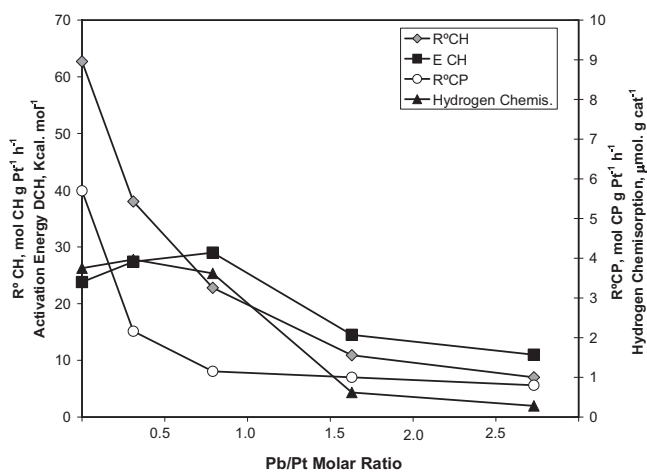


Fig. 8. Values of R_{CH}° and E_{CH} corresponding to CHD, value of R_{CP}° corresponding to CPH, and value of H₂ chemisorption on Pt and PtPb catalysts as a function of the Pb/Pt molar ratio.

of hydrogen chemisorption and the initial rates of test reactions (R_{CH}° and R_{CP}°). The hydrogen chemisorption values for Pb/Pt molar ratios of 0 (corresponding to Pt catalyst), 0.39 (corresponding to 0.1 wt% of Pb) and 0.79 (corresponding to 0.25 wt% of Pb) remain constant as seen in Fig. 8. On the other hand it is observed a strong decrease in R_{CH}° when low Pb contents are added to Pt catalyst. This phenomenon can be explained considering that the cyclohexane dehydrogenation reaction is a structure-insensitive one, and the reagent (CH) is a very large molecule, in comparison with H₂. Hence the accessibility of the cyclohexane molecule to the active sites is lower than that of the hydrogen molecule used for chemisorption experiments. Besides it is observed a stronger decrease of R_{CP}° than R_{CH}° . These results would indicate that the dilution effect of Pb atoms on Pt clusters is more important than blocking one for these

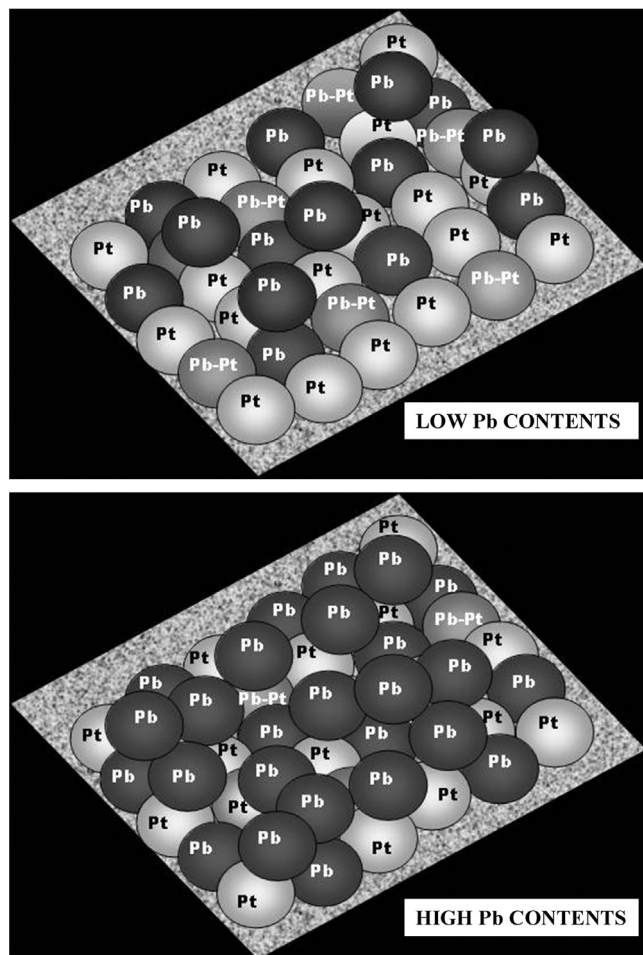


Fig. 9. Models of metallic surface for PtPb catalysts with low and high Pb contents.

catalysts (Pb/Pt molar ratios of 0.39 and 0.79). For high Pb contents, Pb/Pt molar ratios of 1.63 (corresponding to 0.52 wt% of Pb) and 2.73 (corresponding to 0.87 wt% of Pb) respectively, Fig. 8 displays a strong decrease in H_2 chemisorption and R_{CH}° , but the R_{CP}° values for molar ratios of 1.63 and 2.73 are similar to that of a molar ratio of 0.79. These results point to a higher Pb blocking effect than a dilution one in these catalysts with high Pb contents. This conclusion is reinforced by the XPS results (Table 2) that show a high surface enrichment of lead in these samples.

The electronic effects in bimetallic catalysts were analyzed by the modification of the activation energy (E_{CH}) values in CHD with respect to that of Pt catalyst. Fig. 8 shows, for catalysts with Pb/Pt molar ratios of 0.39 and 0.79, an increase in the E_{CH} values respect to the Pt one. This fact together with the higher Pb reducibility to Pb^0 , observed by XPS, indicate the presence of electronic effects of Pb on Pt sites for low amounts of Pb added to Pt catalyst. On the contrary, for catalysts with Pb/Pt molar ratios of 1.63 and 2.73, the E_{CH} values decrease in relation to that of the Pt catalyst. This phenomenon is attributed to the presence of large amounts of Pb (inactive in CHD reaction) blocking the active catalytic surface, in agreement with the important Pb surface enrichment detected by XPS (see Table 2).

In conclusion, for catalysts with low Pb contents, the presence of dilution and electronic effects would produce important improvements in the catalytic behavior of the catalysts, both in activity and in selectivity to olefins (Figs. 1 and 2). In this sense, Palazov et al. [16] found that PtPb system exhibited both the ligand and ensemble effects for low Pb/Pt molar ratios. On the other hand, for catalysts with high Pb contents, the main effect is the blocking of the Pt sites by Pb, such as it was found in previous studies [17,18]. In this sense Cheung et al. [18] found by XPS measurements that there is a strong surface enrichment of Pb on PtPb system, which acts as a poison of the catalytic activity. Hence, from the characterization results we can understand the very poor catalytic behavior of PtPb catalysts with high Pb contents in *n*-butane dehydrogenation, mainly in activity and yield to olefins (Figs. 1 and 3).

Considering the above-mentioned results, models of bimetallic surfaces for low and high Pb contents are displayed in Fig. 9.

3.3. Evaluation of trimetallic catalysts in *n*-butane dehydrogenation reaction

Taking into account that PtPb(0.25 wt%)/MgAl₂O₄ catalyst showed the best catalytic performance in *n*-butane dehydrogenation, two trimetallic catalysts with Pt, Pb and In were prepared with this content of Pb. The promoters (Pb and In) were added to Pt

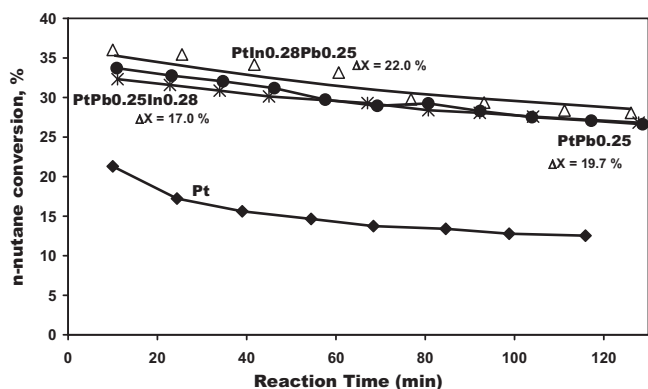


Fig. 10. Values of *n*-butane conversion (X) vs. reaction time and deactivation parameter (ΔX), obtained from flow experiments for Pt, PtPb (with 0.25 wt% of Pb) and PtPbIn catalysts supported on MgAl₂O₄.

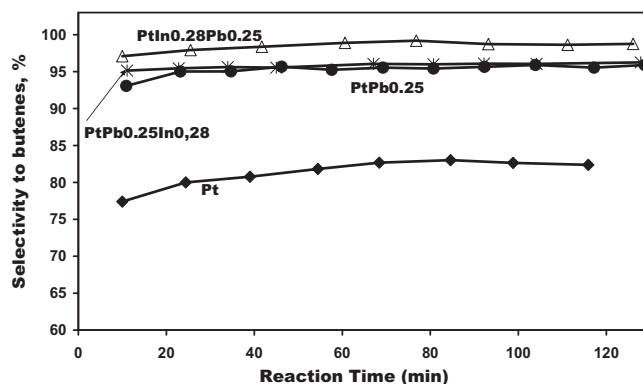


Fig. 11. Selectivity to all butenes (1-butene, *cis*- and *trans*-2-butenes, and 1,3-butadiene) vs. reaction time for Pt, PtPb, and PtPbIn catalysts supported on MgAl₂O₄.

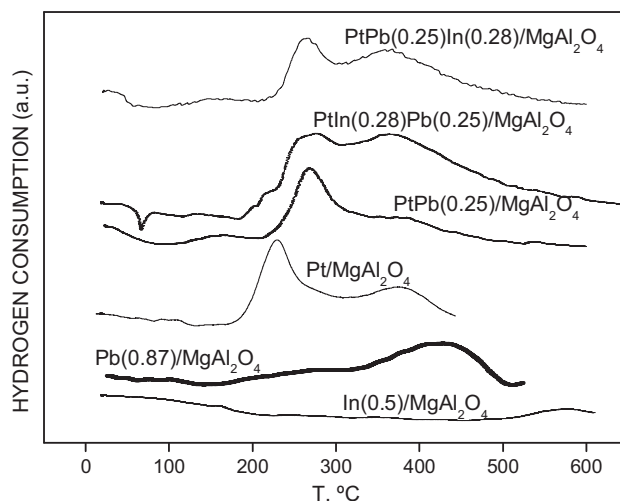


Fig. 12. TPR profiles of calcined Pt, Pb, In, PtPb and PtPbIn catalysts supported on MgAl₂O₄.

catalyst in two different impregnation sequences (see experimental section).

Figs. 10 and 11 show the results of *n*-butane dehydrogenation for trimetallic catalysts compared with those of PtPb and Pt catalysts. The *n*-butane conversion (Fig. 9) of

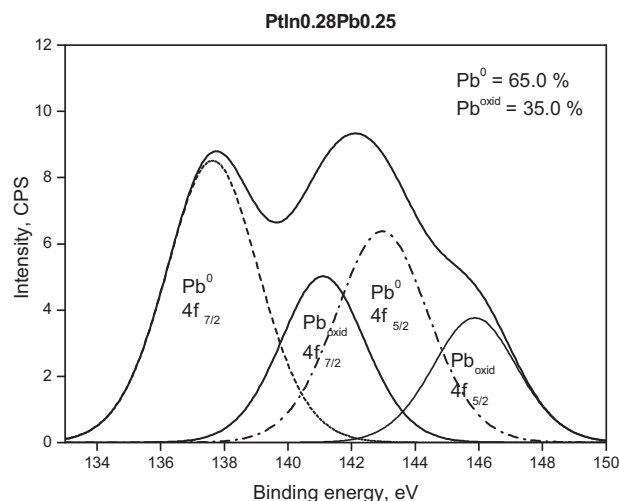


Fig. 13. XPS spectra corresponding to the Pb 4f level for PtIn(0.28 wt%)Pb(0.25 wt%)/MgAl₂O₄ catalyst, previously reduced at 500 °C.

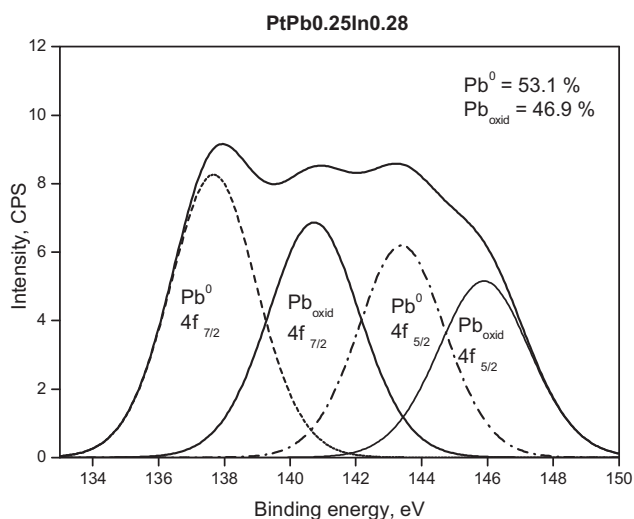


Fig. 14. XPS spectra corresponding to the Pb 4f level for PtPb(0.25 wt%)In(0.28 wt%)/MgAl₂O₄ catalyst, previously reduced at 500 °C.

PtIn(0.28 wt%)Pb(0.25 wt%)/MgAl₂O₄ catalyst is slightly higher than that of the PtPb(0.25 wt%)/MgAl₂O₄ one, while the PtPb(0.25 wt%)In(0.28 wt%)/MgAl₂O₄ exhibits a catalytic activity similar to that of the bimetallic catalyst. Both trimetallic catalysts display similar values of deactivation parameter (ΔX) to that of PtPb(0.25 wt%)/MgAl₂O₄ catalyst. With respect to the selectivity to butenes (Fig. 10) the PtIn(0.28 wt%)Pb(0.25 wt%)/MgAl₂O₄ catalyst displays slightly higher values than the PtPb(0.25 wt%)/MgAl₂O₄ and the PtPb(0.25 wt%)In(0.28 wt%)/MgAl₂O₄ ones. In conclusion, only in the PtIn(0.28 wt%)Pb(0.25 wt%)/MgAl₂O₄ catalyst, the In promoter effect is observed, thus showing the best catalytic performance in *n*-butane dehydrogenation.

3.4. Characterization of metallic phase of trimetallic catalysts

The measurements of H₂ chemisorption in trimetallic catalysts can be observed in the Table 1. The PtPb(0.25 wt%)In

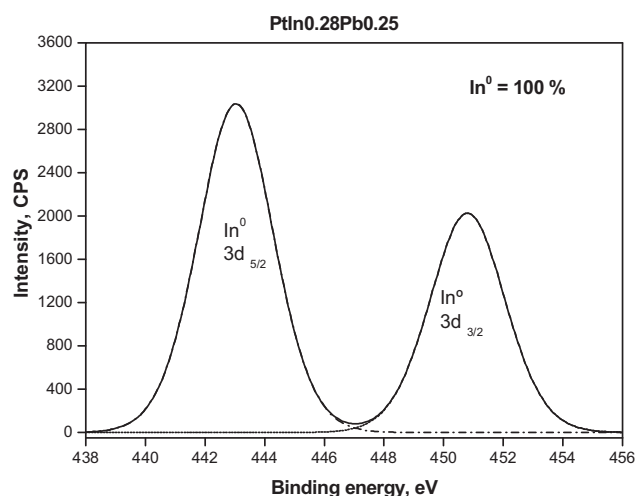


Fig. 15. XPS spectra corresponding to the In 3d level for PtIn(0.28 wt%)Pb(0.25 wt%)/MgAl₂O₄ catalyst, previously reduced at 500 °C.

(0.28 wt%)/MgAl₂O₄ and PtIn(0.28 wt%)Pb(0.25 wt%)/MgAl₂O₄ catalysts display similar values of H₂ chemisorption between them, but lower (about 48%) than that of PtPb(0.25 wt%)/MgAl₂O₄ catalyst. This effect can be due to blocking of the promoters atoms on Pt atoms and/or to electronic effects of the promoters on Pt sites. Table 1 shows the results of CHD and CPH for trimetallic catalysts. The R_{CH}° values for both trimetallic catalysts are much lower than that of the PtPb(0.25 wt%)/MgAl₂O₄ catalyst. This effect would indicate a strong blocking effect of promoters on Pt sites. It must be noted that the activation energy (E_{CH}) values in both trimetallic catalysts could not be evaluated with accuracy due to the low R_{CH}° of these catalysts. Results of CP hydrogenolysis reaction for both trimetallic catalysts display a high dilution effect of promoter atoms on Pt ensembles, since the R_{CP}° values are five times lower than that of the Pt catalyst. In conclusion, in both trimetallic catalysts, geometric effects like blocking and dilution of the of Pt atoms by promoters atoms were detected. Besides, in these catalysts, it

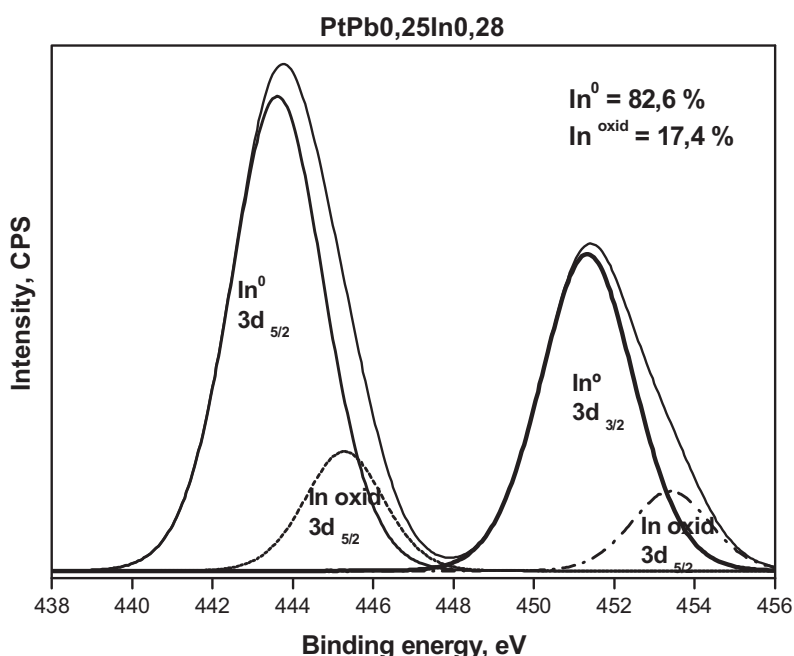


Fig. 16. XPS spectra corresponding to the In 3d level for PtPb(0.25 wt%)In(0.28 wt%)/MgAl₂O₄ catalyst, previously reduced at 500 °C.

could exist electronic effects of metallic promoters on Pt atoms, as it was observed for PtPb(0.25 wt%)/MgAl₂O₄ catalyst.

TPR results of trimetallic catalysts are observed in Fig. 12. Both PtIn (0.28 wt%)Pb(0.25 wt%)/MgAl₂O₄ and PtPb(0.25 wt%)In (0.28 wt%)/MgAl₂O₄ catalysts display an important reduction peak at 265–268 °C, together with a shoulder placed at 360–365 °C. The main reduction zone would correspond to the Pt reduction and also to the co-reduction of oxidized In and Pb species favored by the interaction with Pt. The second reduction zone can be assigned to the reduction of Pb and In isolated species.

XPS results shown in Figs. 13–16 and Table 2 indicate a higher fraction of zerovalent Pb on PtIn (0.28 wt%)Pb(0.25 wt%)/MgAl₂O₄ catalyst compared with PtPb(0.25 wt%)/MgAl₂O₄ and PtPb (0.25 wt%)In (0.28 wt%)/MgAl₂O₄ ones. Besides, the PtIn (0.28 wt%)Pb(0.25 wt%)/MgAl₂O₄ catalyst displays a higher percentage of zerovalent In than in the PtPb(0.25 wt%)In(0.28 wt%)/MgAl₂O₄ one. These results would indicate the presence of electronic effects in PtIn (0.28 wt%)Pb(0.25 wt%)/MgAl₂O₄ catalyst, thus leading to a higher reducibility of both promoters in this sample.

As a summary of the characterization results of trimetallic catalysts, it can be concluded that there are not great differences between the characteristics of the metallic phases of both trimetallic catalysts. However it must be pointed out that the trimetallic catalyst prepared by the sequence (1st Pt, 2nd In, 3rd Pb) presented the highest percentages of Pb⁰ and In⁰ and the best catalytic behavior.

4. Conclusions

At low Pb/Pt molar ratios (0.31 and 0.79), electronic and dilution effects predominate in bimetallic catalysts, thus leading to an improvement of the catalytic performance in *n*-butane dehydrogenation with respect to Pt catalyst. On the other hand, at high Pb/Pt molar ratios (1.63 and 2.73), the main effect is a strong blockage of the surface Pt sites by the second metal. This phenomenon provokes a decrease of the catalytic activity in *n*-butane dehydrogenation compared with the monometallic catalyst, hence Pb in this case poisons the active sites of the catalyst. It must be pointed out that there is an optimum Pb/Pt molar ratio (near to 0.79) to achieve the maximum catalytic yield in this reaction.

The catalytic behavior in *n*-butane dehydrogenation of trimetallic catalysts is influenced by the impregnation sequences of the promoters (Pb and In) to the Pt catalysts. In this sense, only in the PtIn(0.28 wt%)Pb(0.25 wt%)/MgAl₂O₄ catalyst, the promoter effect of In is observed, thus showing the best catalytic performance in the reaction. The characterization results indicate similar effects of blocking and dilution of promoters on active sites of Pt for both trimetallic catalysts, but, the PtIn(0.28 wt%)Pb(0.25 wt%)/MgAl₂O₄

catalyst shows the highest percentages of Pb⁰ and In⁰, which points to a higher interaction between the three metals in this catalyst, compared with the PtPb(0.25 wt%)In(0.28 wt%)/MgAl₂O₄ one. Hence, the influence of the In on the properties of the metallic phase depends on the impregnation sequences of the promoters to Pt catalyst.

Acknowledgements

The authors thank the Secretaría de Ciencia y Técnica – Universidad Nacional del Litoral (CAI+D Program) and ANPCYT for the financial support of this Project. Thanks are also given to Dra. Laura Cornaglia by the collaboration on the interpretation of XPS results, and to Miguel A. Torres by the experimental assistance.

References

- [1] M. Bhasin, J. McCain, B. Vora, T. Imai, P. Pujado, Appl. Catal. A: Gen. 221 (2001) 397–419.
- [2] V.A. Mazzieri, J.M. Grau, C.R. Vera, J.C. Yori, J.M. Parera, C.L. Pieck, Appl. Catal. A: Gen. 296 (2005) 216–221.
- [3] M. Boutzeloito, V.M. Benitez, V.A. Mazzieri, C. Especel, F. Epron, C.R. Vera, C.L. Pieck, P. Marécot, Catal. Commun. 7 (2006) 627–632.
- [4] S.A. Bocanegra, A.A. Castro, A. Guerrero-Ruiz, O.A. Scelza, S.R. de Miguel, Chem. Eng. J. 118 (2006) 161–166.
- [5] A. Ballarini, F. Basile, P. Benito, I. Bersani, G. Fornasari, S. de Miguel, S.P.C. Maina, J. Vilella, A. Vaccari, O.A. Scelza, Appl. Catal. A: Gen. 433–434 (2012) 1–11.
- [6] B.K. Vu, M.B. Song, I.Y. Ahn, Y. Suh, D.J. Suh, W. Kim, H. Koh, Y.G. Choi, E.W. Shin, Appl. Catal. A: Gen. 400 (2011) 25–33.
- [7] A.D. Ballarini, S.A. Bocanegra, A.A. Castro, S.R. de Miguel, O.A. Scelza, Catal. Lett. 129 (2009) 293–302.
- [8] S.A. Bocanegra, A.D. Ballarini, O.A. Scelza, S.R. de Miguel, Mater. Chem. Phys. 111 (2008) 534–541.
- [9] H. Armendáriz, A. Guzmán, J. Toledo, M. Llanos, A. Vazquez, G. Aguilar-Ríos, Appl. Catal. A: Gen. 211 (2001) 69–80.
- [10] S.A. Bocanegra, A. Guerrero-Ruiz, S.R. de Miguel, O.A. Scelza, Appl. Catal. A: Gen. 277 (2004) 11–22.
- [11] T. Ekou, A. Vicente, G. Lafaye, C. Especel, P. Marecot, Appl. Catal. A: Gen. 314 (2006) 64–72.
- [12] F. Passos, M. Schmal, M. Vannice, J. Catal. 160 (1996) 106–116.
- [13] J. Llorca, P. Ramírez de la Piscina, M. Riera, J.L.G. Fierro, J. Sales, N. Homs, J. Mol. Catal. A: Chem. 118 (1997) 101–107.
- [14] S. Göbölös, J. Margitfalvi, M. Hegedüs, Y. Ryndin, React. Kinet. Catal. Lett. 87 (2006) 313–321.
- [15] J. Völter, G. Lietz, M. Ulhemann, M. Hermann, J. Catal. 68 (1981) 42–48.
- [16] A. Palazov, C.H. Bonev, G. Kadinov, D. Shopov, G. Lietz, J. Völter, J. Catal. 71 (1981) 1–9.
- [17] S.A. Bocanegra, M.J. Yañez, O.A. Scelza, S.R. de Miguel, Ind. Eng. Chem. Res. 49 (2010) 4044–4054.
- [18] T.T.P. Cheung, Surf. Sci. Lett. 177 (1986) 493–514.
- [19] A. Cinneide, J. Clarke, Catal. Rev. 7 (1972) 213–232.
- [20] M. Gonzalez-Marcos, B. Iñarra, J. Guil, M. Gutierrez-Ortiz, Appl. Catal. A: Gen. 273 (2004) 259–268.
- [21] M. Boudart, Adv. Catal. 20 (1969) 153–166.
- [22] J.F. Moulder, W.F. Stickle, P.E. Sobol, K.D. Bomben, Handbook of X-ray Photoelectron Spectroscopy, Perkin-Elmer Corp, Eden Prairie, MN, 1992.
- [23] H. Andel-Samad, P.R. Watson, Appl. Surf. Sci. 136 (1998) 46–54.